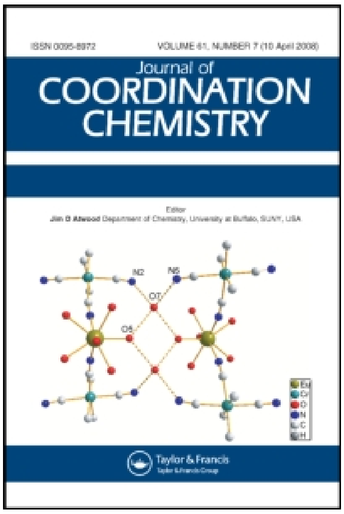

Journal of Coordination Chemistry
Publication details, including instructions for authors and subscription information:
http://www.informaworld.com/smpp/title~content=t713455674

SiF_6^{2-} anionic hydrogen-bonds in $[Co(im)_6]\cdot(SiF_6)\cdot(im)_2$ and *cis*-$[Cd_2(bipy)_2(H_2O)_4(\mu\text{-}F)_2]\cdot SiF_6$ complexes

Jing Wang[a]; Fang-Fang Jian[a]; Xian Wang[a]
[a] New Materials & Function Coordination Chemistry Laboratory, Qingdao University of Science and Technology, Qingdao, 266042, P.R. China

To cite this Article Wang, Jing , Jian, Fang-Fang and Wang, Xian(2009) 'SiF_6^{2-} anionic hydrogen-bonds in $[Co(im)_6]\cdot(SiF_6)\cdot(im)_2$ and *cis*-$[Cd_2(bipy)_2(H_2O)_4(\mu\text{-}F)_2]\cdot SiF_6$ complexes', Journal of Coordination Chemistry, 62: 16, 2623 — 2630, First published on: 24 May 2010 (iFirst)

To link to this Article: DOI: 10.1080/00958970902906276

URL: http://dx.doi.org/10.1080/00958970902906276

Journal of Coordination Chemistry
Vol. 62, No. 16, 20 August 2009, 2623–2630

Taylor & Francis
Taylor & Francis Group

SiF_6^{2-} anionic hydrogen-bonds in $[Co(im)_6]\cdot(SiF_6)\cdot(im)_2$ and *cis*-$[Cd_2(bipy)_2(H_2O)_4(\mu\text{-}F)_2]\cdot SiF_6$ complexes

JING WANG, FANG-FANG JIAN* and XIAN WANG

New Materials & Function Coordination Chemistry Laboratory, Qingdao University of Science and Technology, Qingdao, 266042, P.R. China

(*Received 10 November 2008; in final form 30 December 2008*)

$[Co(im)_6]\cdot(SiF_6)\cdot(im)_2$ (**1**) and *cis*-$[Cd_2(bipy)_2(H_2O)_4(\mu\text{-}F)_2]\cdot SiF_6$ (**2**) [im = imidazole, bipy = 2,2′-bipyridine] have been synthesized and characterized by elemental analysis, IR, UV spectra, and single crystal X-ray diffraction. Crystal data show that two compounds are octahedral and compound **2** is *cis*. Compound **1** displays a layer structure and SiF_6^{2-} bridging hexagram formation by N–H $\cdots$ F–Si interactions between imidazole and SiF_6^{2-}. Compound **2** has two Cds connected by μ-F and O–H $\cdots$ F–S resulting in cave conformation with π–π interactions. For both compounds, SiF_6^{2-} plays an important role in assembling the supramolecular aggregates. The thermal stabilities have also been investigated.

Keywords: Hydrogen-bonds; Fluoride acceptor; μ-F; Anion binding

1. Introduction

Anion binding [1] attracts interest and Bowman-James summarized anion coordination compounds [2, 3]. In frameworks, the counteranion affects the supramolecular architectures through electrostatic interactions and hydrogen bonding. Anions, such as AcO^-, BF_4^-, NO_3^- [4], ClO_4^- [5], SO_3^{2-} [6], and so on, exert dramatic structure-directing behavior, resulting in functional coordination polymers [5]. SiF_6^{2-} either coordinates to metal or fills the vacancy of MOFs, so it is important to understand the influence of SiF_6^{2-} in self-assembly of supramolecular architectures.

SiF_6^{2-} is easily produced even when there is no fluosilicate salt in the synthesis. If there is F^- present in the glass vessel during synthesis, SiF_6^{2-} can be obtained. SiF_6^{2-} in the structure can play an important role in stabilizing supramolecular species. Recently Maekawa and Kitagawa reported SiF_6^{2-} directed the self-assembly of two Ag metallomacrocycles in sandwich-shaped structures [7]. Dong's group reported the crystal structure of $\{[Ag_2(C_{12}H_{10}N_6)_2](SiF_6)\cdot 2H_2O\}_n$ with honeycomb-like channels and found that uncoordinated SiF_6^{2-} and water were located between the layers, further linking by extensive hydrogen-bonding into a 3-D framework [8]. Galet *et al.* demonstrated that the SiF_6^{2-} distributed homogeneously in the interlayer space of

---

*Corresponding author. Email: ffj2003@163169.net

Journal of Coordination Chemistry
ISSN 0095-8972 print/ISSN 1029-0389 online © 2009 Taylor & Francis
DOI: 10.1080/00958970902906276

$[Co(4\text{-terpyridone})_2]\cdot(SiF_6)\cdot nH_2O$ [9]. Kitagawa's group illuminated dynamic SiF_6^{2-} anion exchange properties which accompany structural conversions for $\{[Cu\text{-}(4,4'\text{-bpy})_2(H_2O)_2]\cdot SiF_6\}_n$, in which free SiF_6^{2-} fill microporous channels of dimensions *ca* 2×2 Å^2 [10]. SiF_6^{2-} was included in 3-D porous MOFs built with trinuclear cadmium clusters in a rhombohedral coordination network by Huang *et al.* [11]. More investigations on SiF_6^{2-} binding in coordination frameworks were reported by Zhu and Kitagawa [12], Springsteen *et al.* [13], and Lin *et al.* [14]. In the solid state, electrostatic and hydrogen-bonding interactions of SiF_6^{2-} stabilize the expanded network. However, comparing cation and neutral complexes, study of anion species is still scanty, especially for SiF_6^{2-}.

In this article, we report two compounds, $[Co(im)_6]\cdot(SiF_6)\cdot(im)_2$ and *cis*-$[Cd_2(bipy)_2(H_2O)_4(\mu\text{-}F)_2]\cdot SiF_6$, from reactions with fluoride salts. For both compounds, SiF_6^{2-} links different donor groups by N–H···F–Si and O–H···F–Si hydrogen bonds. Diverse assembling patterns are observed as hexagram formation for **1** and cave structure for **2**.

2. Experimental

2.1. *Materials and physical measurements*

All chemicals were of analytical reagent grade and used directly. HF attacked the glass surface to form SiF_6^{2-} and the presence of SiF_6^{2-} has been confirmed by X-ray analysis. Elemental analyses for carbon, hydrogen, and nitrogen were performed using a Perkin-Elmer 240C elemental instrument. Infrared spectra were recorded on a Nicolet 170SX spectrometer using pressed KBr plates in the range 4000–400 cm^{-1}. UV-Visible absorption spectra were taken with a Purkinje TU-1900 spectrometer, with influences from the quartz liquid cell and DMF solvent subtracted. The weight ratios of Cd and F were obtained by using Inductively Coupled Plasma Torch (ICP) on a VISTA-MPX spectrometer. Thermal gravimetric (TG) and differential analysis (DTA) were recorded on a SDT 2980 simultaneously for 10 mg samples under nitrogen (150 mL min^{-1}) at a heating rate of 10°C min^{-1}.

2.2. *Preparation for $[Co(im)_6]\cdot(SiF_6)\cdot(im)_2$ (1)*

$Co(OH)_2$ was prepared by mixing $Co(NO_3)_2\cdot 6H_2O$ (4.28 g, 20 mmol) with NaOH (1.6 g, 40 mmol) in water. After filtration and washing with water, $Co(OH)_2$ was added to hydrofluoric acid (0.8 g, 40 mmol). The stirring continued until the solid dissolved completely. The CoF_2 solution was obtained after modulating the pH to $5\sim 7$. Ten drops of CoF_2 solution was added to the solution of imidazole (0.13 g, 2 mmol) in 40 mL $EtOH : H_2O = 1:4$. The resulting solution was refluxed for 2 h and filtered. The pink solution obtained was allowed to evaporate slowly, and after several days pink block single crystals were obtained. Anal. Calcd for $C_{24}H_{32}CoF_6N_{14}Si$ (%) **1**: C, 38.62; H, 4.29; N, 26.28. Found: C, 38.60; H, 4.24; N, 26.30. IR (KBr disc ν cm^{-1}): 3141 (N–H), 1460, 1394 (C=N), 752 (Si–F); UV-Vis (DMF) λ_{max} nm (ε dm^{-3} mol^{-1} cm^{-1}): 268 (N–C=N, $n\rightarrow\pi^*$). X-ray crystallographic study has confirmed the existence of $[Co(im)_6]\cdot(SiF_6)\cdot(im)_2$.

2.3. *Preparation for* cis-*[$Cd_2(bipy)_2(H_2O)_4(\mu\text{-}F)_2$]* • *SiF6 (2)*

This complex was prepared as colorless crystals similar to **1**, except for the use of $Cd(NO_3)_2 \cdot 4H_2O$ instead of $Co(NO_3)_2 \cdot 6H_2O$. Anal. Calcd for $C_{20}H_{24}Cd_2F_8N_4O_4Si$ (%) **2**: C, 30.41; H, 3.04; N, 7.09. Found: C, 30.47; H, 3.09; N, 7.04. IR (KBr disc $\nu\,cm^{-1}$): 3394 (C–H), 1440, 1319 (C=N), 750 (Si–F); UV-Vis (DMF) λ_{max} nm ($dm^{-3}\,mol^{-1}\,cm^{-1}$): 283 (interligand, $\pi \rightarrow \pi^*$). Single crystal structure study and ICP data have confirmed the compound is *cis*-[$Cd_2(bipy)_2(H_2O)_4(\mu\text{-}F)_2$] $\cdot$ SiF_6.

2.4. *X-ray investigations*

A summary of the key crystallographic information is given in table 1. Diffraction data were collected on a Bruker SMART diffractometer with graphite-monochromated Mo-Kα radiation ($\lambda = 0.71073$ Å, $T = 293$ K). The technique used was ω-scan with limits 1.39° to 25.49° for **1** and 2.28° to 25.50° for **2**. Empirical absorption correction was carried out by using *SADABS* [15]. The structures were solved by direct methods and refined by least squares on F^2 by using the *SHELXTL* [16] software package. All non-hydrogen atoms were anisotropically refined. The hydrogens of water were located by difference synthesis and refined isotropically and other hydrogens were fixed geometrically at calculated distances and allowed to ride on the parent carbons. For **1**, the final conventional $R_1 = 0.0492$ and $wR_2 = 0.1328$ for 5678 reflections with

Table 1. Crystal data and structure refinement for **1** and **2**.

Complex number	**1**	**2**
Formula weight	745.68	789.32
Temperature (K)	293(2)	293(2)
Wavelength (Å)	0.71073	0.71073
Crystal system, space group	Monoclinic, $P\bar{1}$	Triclinic, $P\bar{1}$
Unit cell dimensions (Å, °)		
a	9.4305(19)	6.7431(2)
b	12.224(2)	9.2081(2)
c	15.749(3)	10.389(2)
α	112.00(3)	101.25(3)
β	90	97.41(3)
γ	90	96.92(3)
Volume (Å^3)	1683.3(5)	620.3(2)
Z, Calculated density ($Mg\,m^{-3}$)	2, 1.471	1, 2.113
Absorption coefficient (mm^{-1})	0.622	1.860
$F(000)$	766	386
Crystal size (mm^3)	0.22 × 0.19 × 0.18	0.24 × 0.21 × 0.17
θ range (°)	1.39 to 24.99	2.28 to 25.50
Limiting indices	$-11 \le h \le 11$, $-6 \le k \le 14$, $-16 \le l \le 17$	$-8 \le h \le 7$, $-8 \le k \le 11$, $-12 \le l \le 12$
Reflections collected/unique	6254/5678 [$R_{int} = 0.0171$]	3388/2280 [$R_{int} = 0.0153$]
Completeness to θ (%)	95.8	98.7
Refinement method	Full-matrix least-squares on F^2	Full-matrix least-squares on F^2
Data/restraints/parameters	5678/0/433	2280/4/182
Goodness-of-fit on F^2	1.043	1.039
Final R indices [$I > 2\sigma(I)$]	$R_1 = 0.0492$, $wR_2 = 0.1328$	$R_1 = 0.0262$, $wR_2 = 0.0693$
R indices (all data)	$R_1 = 0.0547$, $wR_2 = 0.1367$	$R_1 = 0.0272$, $wR_2 = 0.0703$
Largest difference peak and hole ($e\,Å^{-3}$)	0.815 and −0.345	1.224 and −0.643

$I > 2\sigma(I)$ use the weighting scheme, $w = 1/[\sigma^2(F_o^2) + (0.0666P)^2 + 1.2046P]$, where $P = (F_o^2 + 2F_c^2)/3$. For **2**, the final conventional $R_1 = 0.0262$ and $wR_2 = 0.0693$ for 2280 reflections with $I > 2\sigma(I)$ use the weighting scheme, $w = 1/[\sigma^2(F_o^2) + (0.0409P)^2 + 0.7640P]$, where $P = (F_o^2 + 2F_c^2)/3$. The molecular graphics were plotted using SHELXTL. Atomic scattering factors and anomalous dispersion corrections were taken from *International Tables for X-ray Crystallography* [17].

3. Results and discussion

3.1. *Crystal structure of [Co(im)$_6$]•(SiF$_6$)•(im)$_2$ (1)*

X-ray analyses were done at 293 K, 253 K and 203 K (tables 2 and 3). The same crystal cell demonstrates that **1** is stable at low temperature and room temperature. As shown in figure 1(a), **1** is composed of $[Co(im)_6]^{2+}$, two uncoordinated imidazoles and one SiF_6^{2-}. Co in an ideal octahedral geometry is coordinated by six nitrogens from imidazole. Bond lengths and angles are normal for octahedral Co. The dihedral angle of uncoordinated imidazole rings is 13.15°. The shortest Co $\cdots$ Co distance is 9.186 Å. The uncoordinated imidazoles and Si of SiF_6^{2-} are nearly on a plane, the "Si–im" layer, with mean deviation from the best plane of 0.192 Å.

The crystal structure of **1** shows strong intramolecular hydrogen-bonding interactions N–H $\cdots$ N between uncoordinated imidazole rings [distance of N(13) $\cdots$ N(13), N(14) $\cdots$ N(16), N(16) $\cdots$ N(15) are all 2.854(2) Å, N(15) $\cdots$ N(15) = 2.907(3) Å]. The fluorides [F(1) and F(5)] of SiF_6^{2-} each have two N–H $\cdots$ F interactions, whereas F(2), F(3), and F(4) have two strong N–H $\cdots$ F contacts and the weak C–H $\cdots$ F. F(6) has four contacts with the surrounding imidazole *via* two C–H $\cdots$ F and two N–H $\cdots$ F hydrogen bonds. The distances and angles observed for C–H $\cdots$ F and N–H $\cdots$ F are

Table 2. Selected bond lengths (Å) and angles (°) of **1** and **2**.

$[Co(im)_6] \cdot (SiF_6) \cdot (im)_2$ (**1**)		*cis*-$[Cd_2(bipy)_2(H_2O)_4(\mu\text{-}F)_2] \cdot SiF_6$ (**2**)	
Co(1)–N(11)	2.161(2)	Cd(1)–N(1)	2.317(3)
Co(1)–N(7)	2.165(2)	Cd(1)–F(1)	2.240(2)
Co(1)–N(9)	2.169(2)	Cd(1)–O(2W)	2.271(3)
N(11)–Co(1)–N(7)	89.75(9)	Cd(1)–O(1W)	2.289(3)
N(3)–Co(1)–N(7)	90.69(9)	F(1)–Cd(1)$^{\#1}$	2.226(2)
N(11)–Co(1)–N(5)	179.50(9)	F(1)$^{\#1}$–Cd(1)–F(1)	76.75(8)
N(7)–Co(1)–N(5)	90.68(9)	F(1)$^{\#1}$–Cd(1)–O(2W)	86.56(9)
N(3)–Co(1)–N(1)	89.49(9)	F(1)–Cd(1)–O(2W)	160.50(1)
N(7)–Co(1)–N(9)	88.30(9)	F(1)$^{\#1}$–Cd(1)–O(1W)	104.27(1)
N(5)–Co(1)–N(9)	90.04(9)	F(1)–Cd(1)–O(1W)	92.23(9)
		O(2W)–Cd(1)–O(1W)	82.07(1)
		F(1)–Cd(1)–N(2)	92.35(9)
		O(2W)–Cd(1)–N(2)	98.36(1)
		O(1W)–Cd(1)–N(2)	163.55(1)
		F(1)–Cd(1)–N(1)	103.11(9)
		O(2W)–Cd(1)–N(1)	95.80(1)
		O(1W)–Cd(1)–N(1)	92.68(1)
		Cd(1)$^{\#1}$–F(1)–Cd(1)	103.25(8)

Symmetry transformations used to generate equivalent atoms: #1: $= -x + 1$, $-y + 2$, $-z$.

within the range reported in the literature [18]. The N–H$\cdots$F interactions result in 12 contacts between imidazole and SiF_6^{2-}.

The N–H$\cdots$N intramolecular hydrogen bonds between uncoordinated imidazoles create a 1-D wave chain, the "im–im chain". SiF_6^{2-} anions are at each crook of im–im chains (figure 1b). "im-Si" layer and SiF_6^{2-} counterion are fixed by C–H$\cdots$F interactions. An infinite layered packing mode is shown in figure 1(c). Each layer, constructed by two "Si–im" sheets and $[Co(im)_6]^{2+}$ host, assemble into an infinite extended hydrogen-bonding network over the entire *ac*-plane. The distance between two layers is *ca* 11.153 Å. Figure 1(d) shows the perfect hexagram, in which SiF_6^{2-} is located on the center. The 12 N$\cdots$F–Si links connect the layers and $[Co(im)_6]^{2+}$ host. SiF_6^{2-} hydrogen bonds with different donors to enhance crystal stability.

3.2. *Crystal structure of* cis-$[Cd_2(bipy)_2(H_2O)_4(\mu\text{-}F)_2]\cdot SiF_6$ *(2)*

The structure of **2** is distinct from **1** (figure 2a), consisting of a central $Cd_2F_2O_4N_4$ core and a SiF_6^{2-}. Each Cd is in distorted octahedral geometry with two N atoms, two O atoms and two F atoms. O and F atoms each are *cis*. Two F^- bridge two Cds forming a dimer. A $(\mu\text{-}F)_2Cd$ structure was only reported by Tomat *et al.* [19], Ouellette *et al.* [20], and Reger *et al.* [21]. The coordination environment of Cd is completed by 2,2′-bipyridine at 2.317(3) and 2.310(3) Å, μ-F at 2.240(2) and 2.226(2) Å and two water molecules at 2.289(3) and 2.271(3) Å. The Cd–F distance is shorter than that reported for $C_8As_4Cd_2F_{36}N_{20}S_{12}$ [2.475 Å and 2.566 Å] [22]. Other distances are similar to

Table 3. Table of hydrogen-bond interactions of **1** and **2**.

Donor–H$\cdots$Acceptor	Symm	D–H (Å)	H$\cdots$A (Å)	D$\cdots$A (Å)	D–H$\cdots$A (°)
$[Co(im)_6]\cdot(SiF_6)\cdot(im)_2$					
N(2)–H(2A)$\cdots$F(2)	1 + *x*, 1 + *y*, *z*	0.860	2.052	2.867	157.95
N(2)–H(2A)$\cdots$F(3)	1 + *x*, 1 + *y*, *z*	0.860	2.304	2.946	131.60
N(4)–H(4A)$\cdots$F(1)	1 + *x*, *y*, *z*	0.860	2.150	2.856	139.07
N(4)–H(4A)$\cdots$F(5)	1 + *x*, *y*, *z*	0.860	2.117	2.896	150.37
N(6)–H(6A)$\cdots$F(1)	1−*x*, 1−*y*, −*z*	0.860	2.313	3.044	143.02
N(6)–H(6A)$\cdots$F(4)	1−*x*, 1−*y*, −*z*	0.860	2.064	2.840	149.69
N(8)–H(8A)$\cdots$F(4)		0.860	2.097	2.916	158.74
N(8)–H(8A)$\cdots$F(5)		0.860	2.280	2.958	135.76
N(10)–H(10A)$\cdots$F(3)	*x*, 1 + *y*, *z*	0.860	2.069	2.868	154.24
N(10)–H(10A)$\cdots$F(6)	*x*, 1 + *y*, *z*	0.860	2.190	2.887	137.89
N(12)–H(12A)$\cdots$F(2)	1−*x*, 1−*y*, 1−*z*	0.860	2.361	3.065	139.34
N(12)–H(12A)$\cdots$F(6)	1−*x*, 1−*y*, 1−*z*	0.860	2.062	2.854	152.68
C(19)–H(19A)$\cdots$F(2)	−*x*, 1−*y*, 1−*z*	0.930	2.477	3.261	142.03
C(20)–H(20A)$\cdots$F(6)	1−*x*, 1−*y*, 1−*z*	0.930	2.422	3.238	146.49
C(23)–H(23A)$\cdots$F(4)		0.930	2.523	3.233	133.38
C(23)–H(23A)$\cdots$F(6)		0.930	2.418	3.335	168.65
C(24)–H(24A)$\cdots$F(3)	1−*x*, −*y*, −*z*	0.930	2.488	3.400	166.73
cis-$[Cd_2(bipy)_2(H_2O)_4(\mu\text{-}F)_2]\cdot SiF_6$					
O(1W)–H(11W)$\cdots$F(2)	*x*, 1 + *y*, *z*	0.845	1.921	2.721	157.52
O(2W)–H(12W)$\cdots$F(3)	−*x*, 1−*y*, 1−*z*	0.844	1.815	2.654	172.85
O(1W)–H(21W)$\cdots$F(4)	1−*x*, 1−*y*, 1−*z*	0.846	2.096	2.887	155.34
O(2W)–H(22W)$\cdots$F(1)	−1 + *x*, *y*, *z*	0.847	1.803	2.613	159.53
C(4)–H(4A)$\cdots$F(1)	1−*x*, 1−*y*, −*z*	0.930	2.520	3.303	141.98

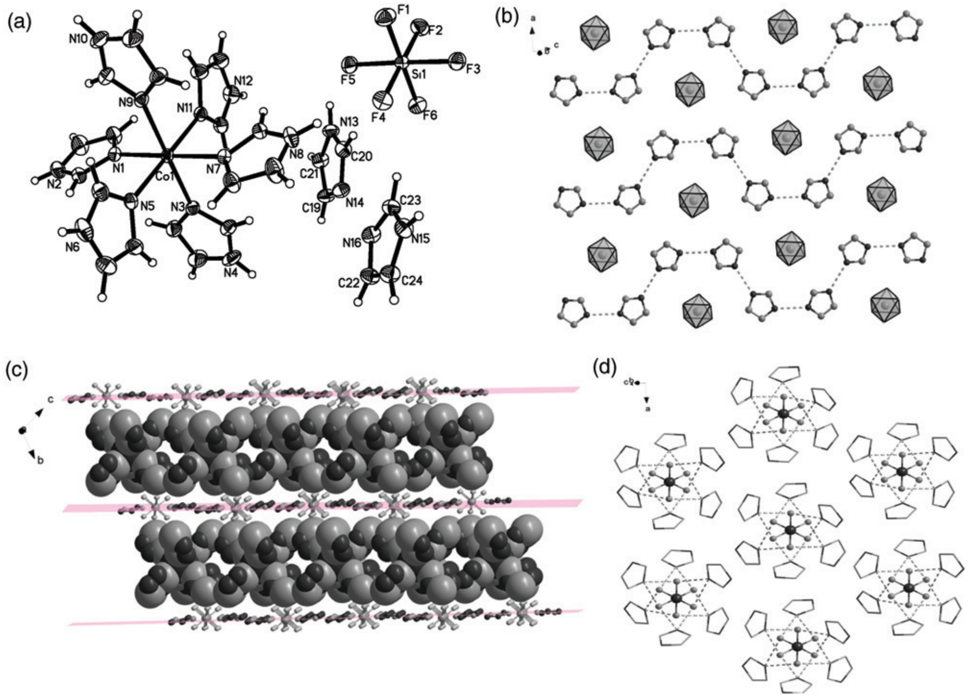

Figure 1. (a) Structure of **1** showing 30% probability displacement ellipsoids and the atom-numbering scheme. (b) A view of im–im wave chains and SiF_6^{2-} (hydrogen atoms are omitted for clarity). (c) Infinitely extended layer-packing mode; the thickness of the stacked units in a layer is 11.153 Å. Hydrogen atoms not related to coordination imidazole are omitted for clarity. The $[Co(im)_6]^{2+}$ host is represented in the space fill mode, while other groups are represented in the standard ball and stick mode. (d) Hexagram framework formed by N–H $\cdots$ F–Si hydrogen bonding.

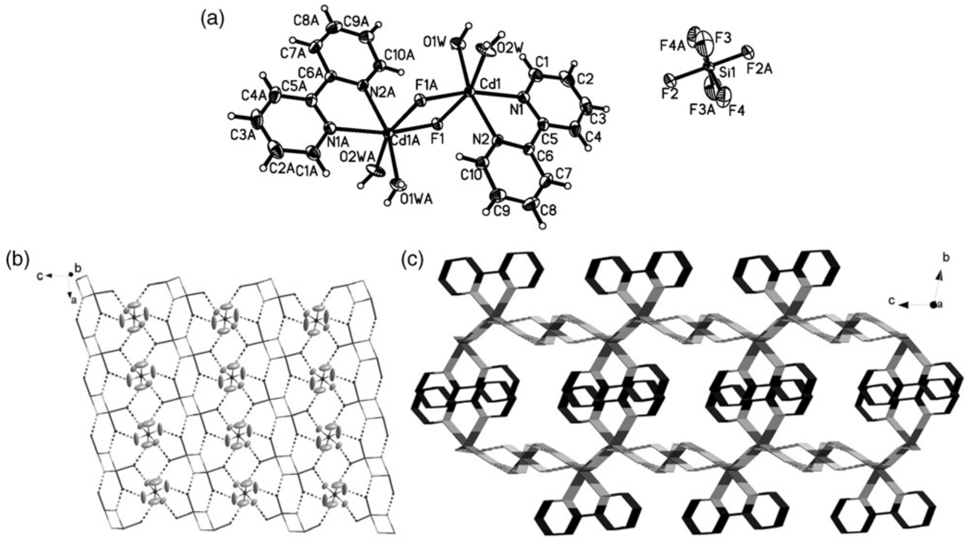

Figure 2. (a) Structure of **2** showing 30% probability displacement ellipsoids and the atom-numbering scheme. (b) 2-D network of O–H $\cdots$ F hydrogen bonds through the intermolecular O–H $\cdots$ F hydrogen bonds (C, H and N atoms are omitted for clarity). (c) The cave framework formed by O–H $\cdots$ F hydrogen bonds and π–π stacking interactions.

previously described [23–25]. The O(1w)–Cd–F(1) angle is 92.23° and O(2w)–Cd–F(1) is 160.50°. The dihedral angle between ring 1 [Cd(1)–F(1)–Cd(1b)–F(1b)] and ring 2 [Cd(1)–N(1)–C(5)–C(6)–N(2)] is 89.38°.

The crystal packing is dominated by two strong hydrogen bonds. All fluorides contact with two coordination water molecules [O(1W)$\cdots$F(2) = 2.7212 Å, O(2W)$\cdots$F(3) = 2.6540 Å, O(1W)$\cdots$F(4) = 2.8867 Å, O(2W)$\cdots$F(1) = 2.6131 Å], and fluoride F(1) with carbon atom [C(4)$\cdots$F(1) = 3.3028 Å]. There are two types of C–H$\cdots\pi$ supramolecular interactions between carbon with ring 1 [Cd(1)–F(1)–Cd(1b)–F(1b)] and ring 2 [Cd(1)–N(1)–C(5)–C(6)–N(2)] [C(4)–H(4A)$\cdots$Cg(2) = 3.363 Å, C(10)–H(10A)$\cdots$Cg(1) = 2.977 Å]. The π–π stacking exists between two bipyridine rings [N(1), C(1)~C(5)] and [N(2), C(6)~C(10)] of the ligand in the crystal lattice (dihedral angle 4.21°, centroid–centroid separation 3.543 Å). Crystal packing is directed by electrostatic forces, hydrogen bonds and π–π stacking interactions.

The $Cd_2F_2O_2$ units form a step-like chain in the direction of *c*-axis, *via* hydrogen bond of coordinated fluoride and water. Six fluorides of SiF_6^{2-} associate directly to lateral chains by O–H$\cdots$F hydrogen bonds. The 2-D supramolecular network is shown in figure 2(b). Each SiF_6^{2-} is surrounded by four hosts having six hydrogen-bonding contacts. Every fluoride of SiF_6^{2-} links one coordinated water molecule. The architecture is a 3-D cave framework constructed by O–H$\cdots$F–Si hydrogen bonds and π–π interactions between pyridine rings (figure 2c).

3.3. *Thermal analysis*

The TG/DSC curves of **1** and **2** are presented in "Supplementary material". Thermal decomposition of **1** includes four endothermic peaks (121.3, 174.2, 226.2, 548.1°C). From 121.3 to 254.4°C, all imidazole rings decompose with three weight losses; the residue may be $Co(NH_3)_2SiF_6$ (found: 68.79%; Calcd: 68.39%). Of course, we do not determine the exact formula of the residue, but, in the temperature range of 254 ~ 420°C, there is a flat line with no weight loss observed, suggesting the residue is stable during this temperature range. Thus, $[Co(NH_3)_2SiF_6]$ can be obtained if we heat **1** under inert-gas or vacuum at about 300°C for several hours. The thermal decomposition process of **2** can be divided into two stages at 179.9 and 268.7°C. The first weight loss corresponds to loss of four coordinated water molecules (found: 10.18%; Calcd: 9.12%), with an intense endothermic phenomenon; the residue may be *cis*-$[Cd_2(bipy)_2(\mu\text{-}F)_2]\cdot SiF_6$. The second weight loss may be the loss of 2,2′-bipyridine and two fluorides (found: 51.43%, Calcd: 51.96%). Between 280 and 480°C, the stable $CdSiF_6$ exists.

4. Conclusions

The structure clearly demonstrates that SiF_6^{2-} as the acceptor plays an important role in the supramolecular framework by hydrogen bonds. SiF_6^{2-} anion sits on the hexagram center and connects $[Co(im)_6]^{2+}$ with layer structure in **1**. For **2**, donor attached to fluoride of SiF_6^{2-} forms strong hydrogen bonds and plays the key role in formation of chains and 3-D framework.

Supplementary material

Crystallographic data for the structural analyses have been deposited with the Cambridge Crystallographic Data Centre. CCDC-688641 for **1** and CCDC-669358 for **2** contain the supplementary crystallographic data for this article. These data can be obtained free of charge from the Cambridge Crystallographic Data Centre *via* www.ccdc.cam.ac.uk/data_request/cif.

Acknowledgment

The authors would like to thank Natural Science Foundation of Shandong Province (No. Y2005B04 and No. Z2007B01), P.R. China.

References

[1] P.S. Lakshminarayanan, E. Suresh, P. Ghosh. *Inorg. Chem.*, **45**, 4372 (2006).
[2] (a) B. Wu, X.J. Huang, Y.Z. Xia, X.J. Yang, C. Janiak. *CrystEngComm.*, **9**, 676 (2007); (b) M.A. Hossain, P. Morehouse, D. Powell, K. Bowman-James. *Inorg. Chem.*, **44**, 2143 (2005).
[3] K. Bowman-James. *Acc. Chem. Res.*, **38**, 671 (2005).
[4] D.K. Kumar, A. Das, P. Dastidar. *CrystEngComm.*, **9**, 548 (2007).
[5] S.M. Krishnan, N.M. Patel, W.R. Knapp, R.M. Supkowski, R.L. LaDuca. *CrystEngComm.*, **9**, 503 (2007).
[6] L.M. Wu, H.B. Teng, X.C. Feng, X.B. Ke, Q.-F. Zhu, J.-T. Su, W.-J. Xu, X.-M. Hu. *Cryst. Growth Des.*, **7**, 1337 (2007).
[7] M. Maekawa, S. Kitagawa, T. Kuroda-Sowa, M. Munakata. *Chem. Commun.*, 2161 (2006).
[8] Y.-B. Dong, H.-Y. Wang, J.-P. Ma, R.-Q. Huang, M.D. Smith. *Cryst. Growth Des.*, **5**, 789 (2005).
[9] A. Galet, A.B. Gaspar, M.C. Munoz, J.A. Real. *Inorg. Chem.*, **45**, 4413 (2006).
[10] S. Noro, R. Kitaura, M. Kondo, S. Kitagawa, T. Ishii, H. Matsuzaka, M. Yamashita. *J. Am. Chem. Soc.*, **124**, 2568 (2002).
[11] Y.-Q. Huang, B. Ding, H.-B. Song, B. Zhao, P. Ren, P. Cheng, H.-G. Wang, D.-Z. Liao, S.-P. Yan. *Chem. Commun.*, 4906 (2006).
[12] L.-G. Zhu, S. Kitagawa. *Inorg. Chem. Commun.*, **5**, 358 (2002).
[13] C.H. Springsteen, R.D. Sweeder, R.L. LaDuca. *Cryst. Growth Des.*, **6**, 2308 (2006).
[14] P. Lin, R.A. Henderson, R.W. Harrington, W. Clegg, C.-D. Wu, X.-T. Wu. *Inorg. Chem.*, **43**, 181 (2004).
[15] G.M. Sheldrick. *Acta Crystallogr., Sect. A*, **46**, 467 (1969).
[16] G.M. Sheldrick. *SHELXTL97, Program for Crystal Structure Refinement*, University of Gottingen, Germany (1993).
[17] A.J. Wilson. *International Table for X-ray Crystallography*, Vol. C, Tables 6.1.1.4, pp. 500–502 and 4.2.6.8, pp. 219–222, Kluwer Academic Publishers, Dordrecht (1992).
[18] C.A. Ilioudis, D.A. Tocher, J.W. Steed. *J. Am. Chem. Soc.*, **126**, 12395 (2004).
[19] E. Tomat, L. Cuesta, V.M. Lynch, J.L. Sessler. *Inorg. Chem.*, **46**, 6224 (2007).
[20] W. Ouellette, B.S. Hudson, J. Zubieta. *Inorg. Chem.*, **46**, 4887 (2007).
[21] D.L. Reger, R.P. Watson, J.R. Gardinier, M.D. Smith, P.J. Pellechia. *Inorg. Chem.*, **45**, 10088 (2006).
[22] C. Knapp, R. Mews. *Eur. J. Inorg. Chem.*, 3536 (2005).
[23] X.-D. Chen, J.-H. Guo, M. Du, T.C.W. Mak. *Inorg. Chem. Commun.*, **8**, 766 (2005).
[24] R.H. Laye, F.K. Larsen, J. Overgaard, C.A. Muryn, E.J.L. McInnes, E. Rentschler, V. Sanchez, S.J. Teat, H.U. Güdel, O. Waldmann, G.A. Timco, R.E.P. Winpenny. *Chem. Commun.*, 1125 (2005).
[25] F.K. Larsen, E.J.L. McInnes, H.E. Mkami, J. Overgaard, S. Piligkos, G. Rajaraman, E. Rentschler, A.A. Smith, G.M. Smith, V. Boote, M. Jennings, G.A. Timco, R.E.P. Winpenny. *Angew. Chem., Int. Ed. Engl.*, **42**, 101 (2003).